Supplementary Information (SI) for Journal of Materials Chemistry C.

Supporting Information

A highly sensitive MOF fluorescence probe for discriminative detection of aliphatic and aromatic amines

Changjiang Zhou,[a] Yafei Liu,[a] Zimeng Liu,[a] Zhichao Qiu,[a] Zhuangzhuang Sun,[a] Minrui Chen,[a] Bo Xie,[a] Hui-min Wen,[a] Jun Hu*[a]

[a] College of Chemical Engineering, Zhejiang University of Technology, Hangzhou 310014, P. R. China

Contents

S-I Characterization and Measurements

S-II Figures

S-III Tables

S-IV References

S-I Characterization and Measurements

Instrument: The structure and morphology of lanthanide Metal−Organic Framework were characterized by a Hitachi S-4700 scanning electron microscope (Japan, Hitachi). UV-vis absorption spectra were collected using a TU-1900 by Beijing Purkinje GENERAL Instrument Co., Ltd.. Fluorescence spectra were measured using an F-2700 fluorescence spectrophotometer (Japan, Hitachi) with a photomultiplier tube (PMT) voltage fixed at 400 V, excitation and emission slits set at 5 nm, and the scanning speed is set to 1500 nm·min^{-1}. Solid powder X-ray diffraction analysis was shown using an Empyrean type X-ray powder diffractometer (Dutch, PNAlytical). Fourier transform infrared (FT-IR) spectroscopy was recorded using a Nicolet IS50 micro-infrared spectrometer (America, Thermo). Thermal gravimetric analysis (TGA) was undertaken on a TGA/DSC Model 3+ Simultaneous Thermal Analysis Mass Spectrometer at a heating rate of 10 °C min^{-1}. The electronic properties of the elements in the MOF were analyzed by XPS (Thermo- -ESCALAB250). The room-temperature lifetimes were measured on an Edinburgh FLS-980 with an EPL-375 optical laser. Nitrogen adsorption-desorption measurements were conducted using a Micromeritics 3Flex surface characterization analyzer. Specific surface areas were calculated by the Brunauer-Emmett-Teller (BET) method.

Materials: Europium chloride hexahydrate ($EuCl_3 \cdot 6H_2O$), 1,2-diaminobenzene(OPD) and m-Phenylenediamine(MPD) were bought from Shanghai Adamas Reagent Co., Ltd. (Shanghai, China). Pyridine dicarboxylic acid (2, 6-pyridine dicarboxylic acid, DPA) and diethylamine (DEA) were bought from Aladdin Reagent Co., Ltd (Shanghai, China). Ethanol absolute, ethylenediamine(EDA), and triethylamine (TEA) were purchased from Sinopharm Chemical Reagent Co., Ltd. (Shanghai, China) p-phenylenediamine (PPD), ethylamine (EA), and aniline (AN) were purchased from Shanghai Macklin Biochemical Co. Ltd. (Shanghai, China). All the medicines and reagents used in the experiment were analytically pure, and the water used in the experiment was ultrapure water of 18.25 MΩ/cm.

***Detection of Amines by Eu-DPA*:** All the fluorescence titration measurements were conducted by exciting the resulting suspension at 275 nm and recording the spectra within 295-800 nm. To perform the concentration-dependent sensing event, Eu-DPA was ground into a fine powder and uniformly dispersed in 2 mL mili-Q water to prepare a 0.5 mg·mL^{-1} Eu-DPA solution. Sonication resulted in a homogeneous suspension, followed by the addition of varying amounts of hydrazine hydrate. After standing for a while, the resulting suspension was transferred to a cuvette. Fluorescence emission spectra were collected at room temperature, and conditions were kept constant for each fluorescence test.

Computational Methods: All the density functional theory (DFT) calculations were performed with Gaussian 09 (version D.01) package on a PowerLeader cluster.

Geometries of compounds DEA, EA, TEA, EDA, AN, OPD, MPD, PPD and DPA were optimized with B3LYP hybrid functional at the basis set level of 6-31G(d, p). The highest occupied molecular orbital (LUMO) energies and the lowest unoccupied molecular orbital (LUMO) energies of the DEA, EA, TEA, EDA, AN, OPD, MPD, PPD and DPA were then obtained from the output files. Based on optimized geometries, the excited state properties were estimated by time-dependent density functional theory (TD-DFT) with the B3LYP functional at the same basis.

Preparation of Eu-DPA test strips**:** Luminescence test strips were fabricated by immersing qualitative filter paper in a 0.5 mg/mL Eu-DPA ethanol suspension using the dipping method. The filter paper was cut into rectangular pieces and soaked in the solution for 10 hours. Afterward, the paper was vacuum-dried at 60 °C overnight, yielding the Eu-DPA test strips.

Cyclic Testing: The Eu-DPA aqueous suspension treated with DEA/PPD was filtered, repeatedly washed with distilled water, and dried before conducting each subsequent sensing experiment.

S-II Figures

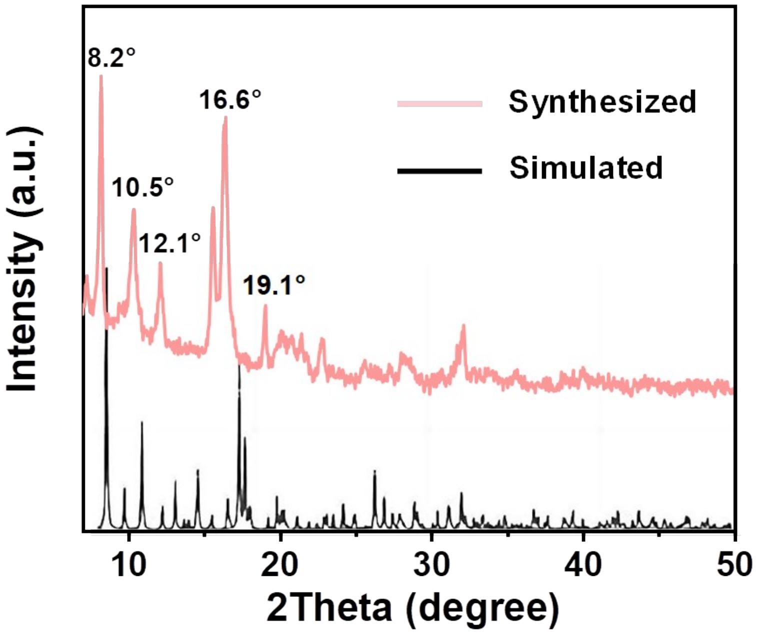

Figure S1. PXRD patterns of synthesized and simulated Eu-DPA.

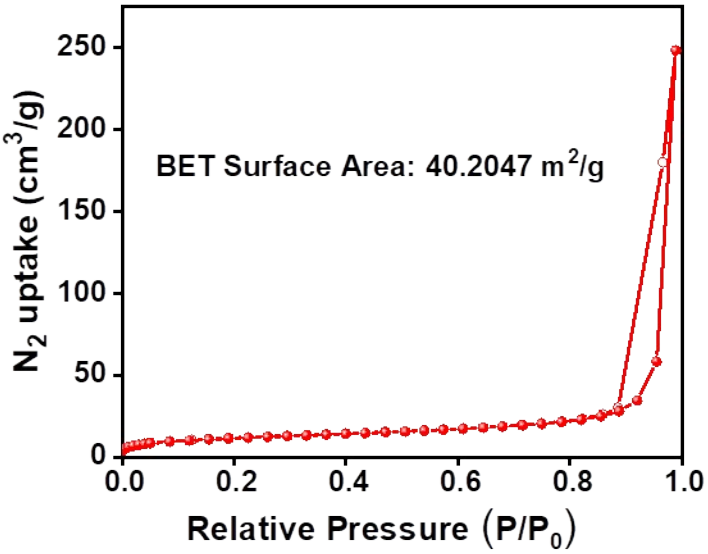

Figure S2. N_2 adsorption/desorption isotherms of Eu-DPA recorded at −195.85 °C.

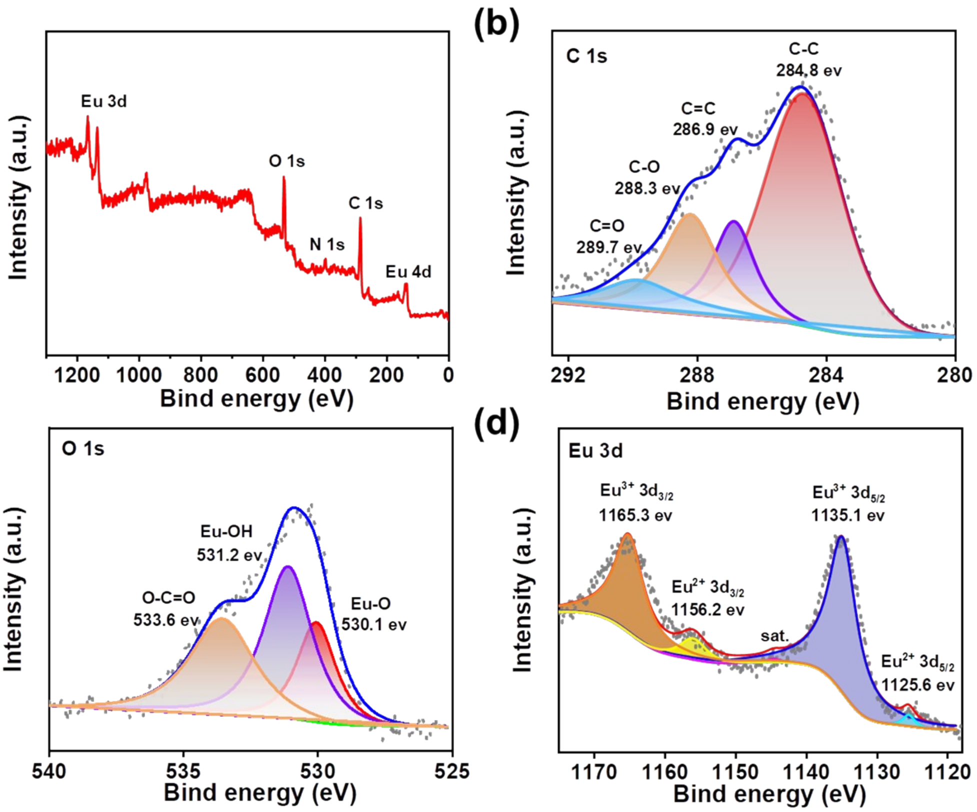

Figure S3. XPS survey spectra (a), C 1s (b), O 1s (c) and Eu 3d (d) of Eu-DPA.

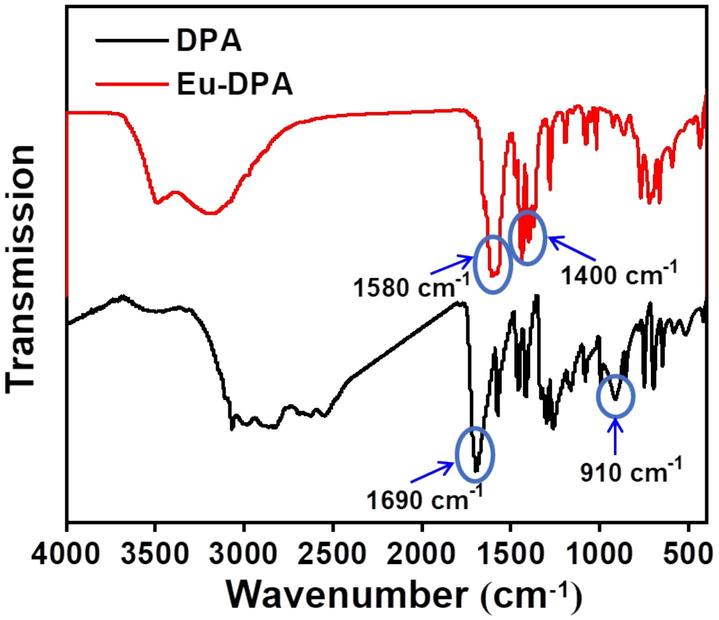

Figure S4. FT-IR spectra of DPA and Eu-DPA.

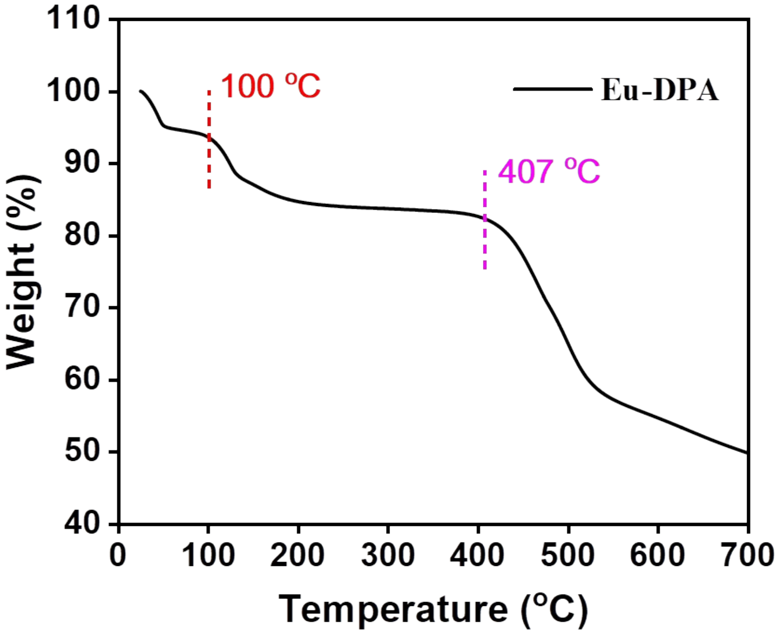

Figure S5. The thermal gravimetric analysis of Eu-DPA.

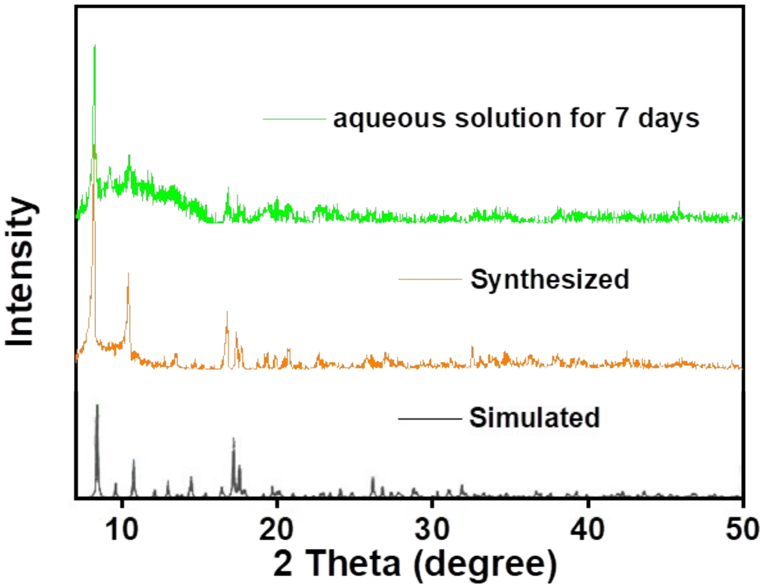

Figure S6. PXRD patterns of Eu-DPA after soaked in aqueous solution for 7 days.

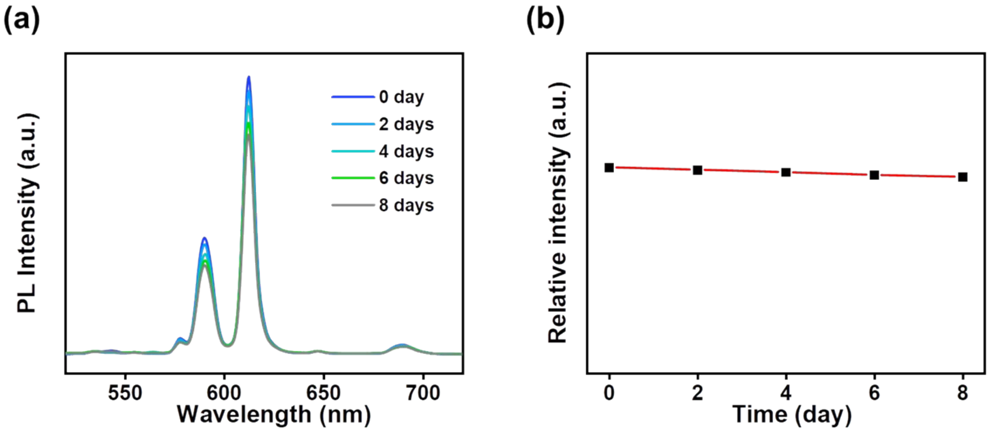

Figure S7. PL spectra and intensities of Eu-DPA after soaked in aqueous solution for different days.

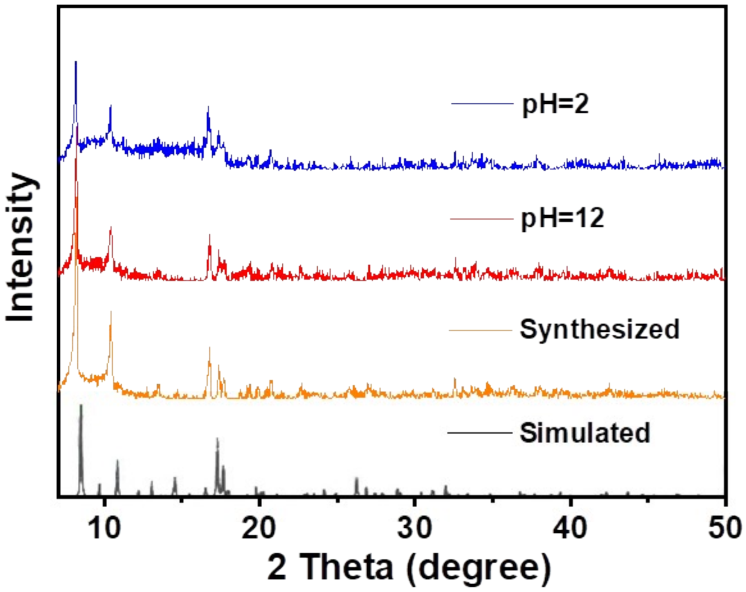

Figure S8. PXRD patterns of Eu-DPA after treatment with acidic (pH=2) and basic (pH=12) aqueous solutions.

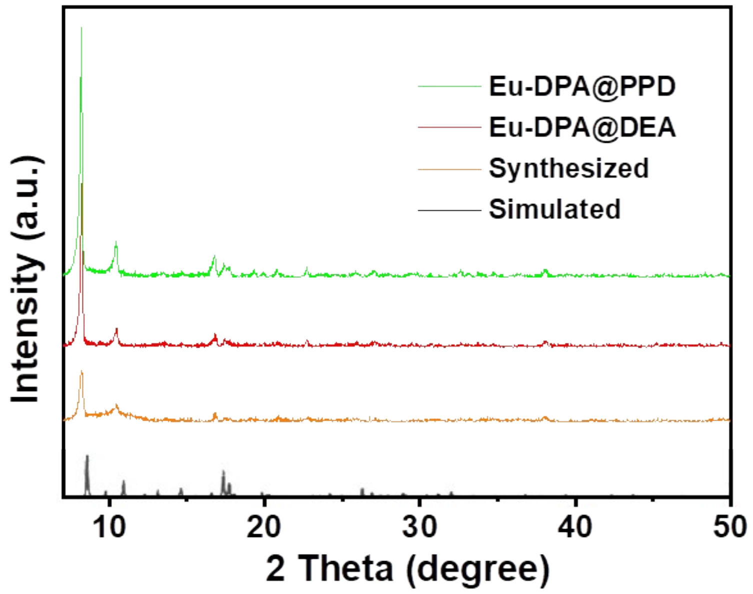

Figure S9. PXRD patterns of Eu-DPA after treatment with DEA and PPD solutions.

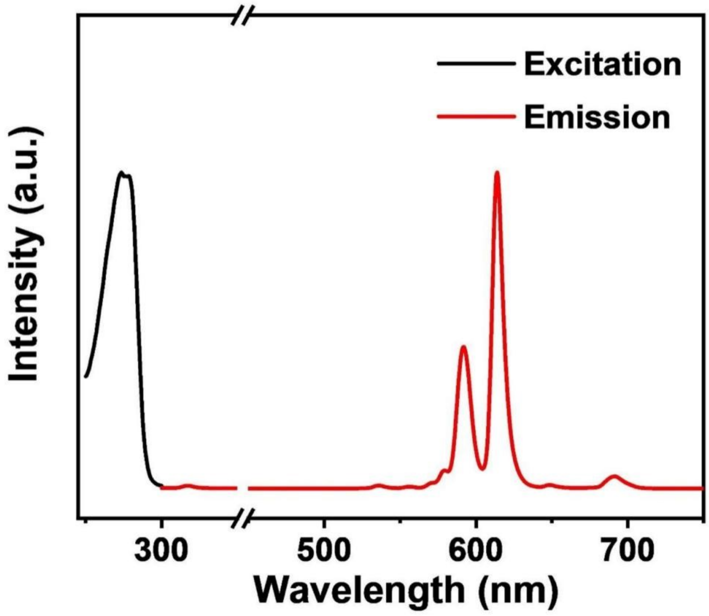

Figure S10. The excitation (λ_{ex}=275 nm, black line) and emission (λ_{em} =614 nm, red solid line) spectra of Eu-DPA.

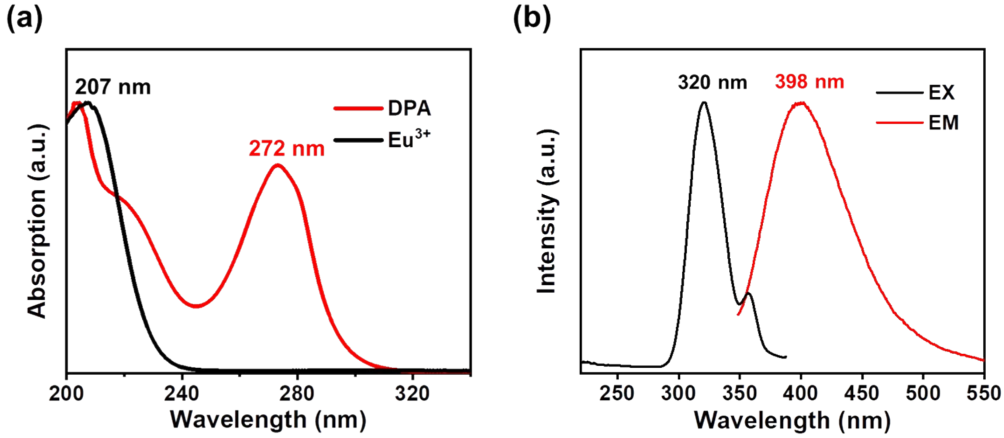

Figure S11. (a)The UV-vis absorption spectra of DPA and Eu^{3+}; (b) the excitation and emission spectra of DPA.

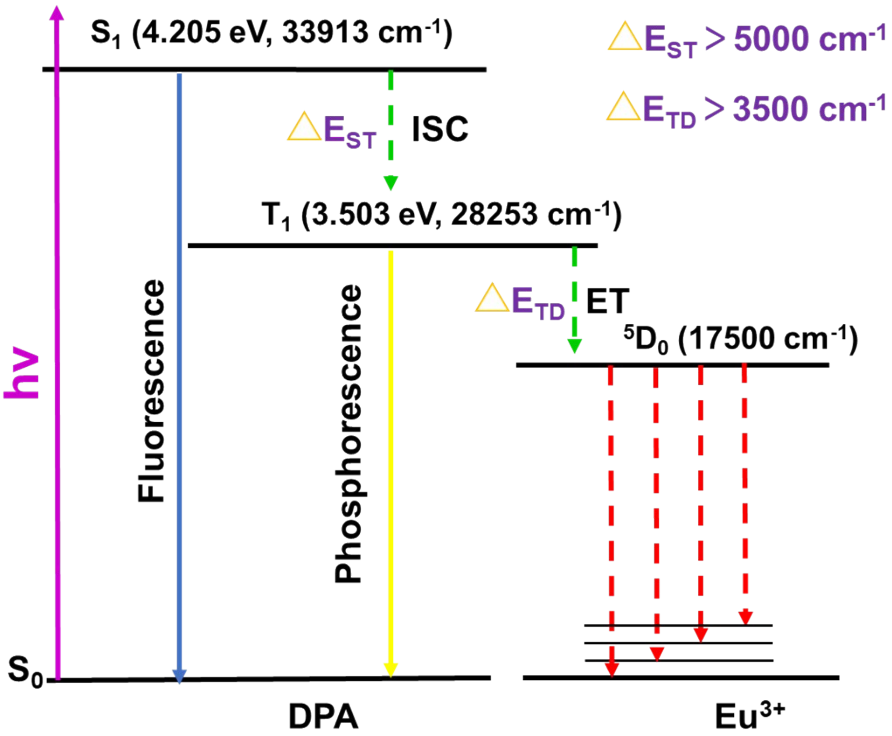

Figure S12. The energy level schematic diagram of DPA and Eu^{3+}.

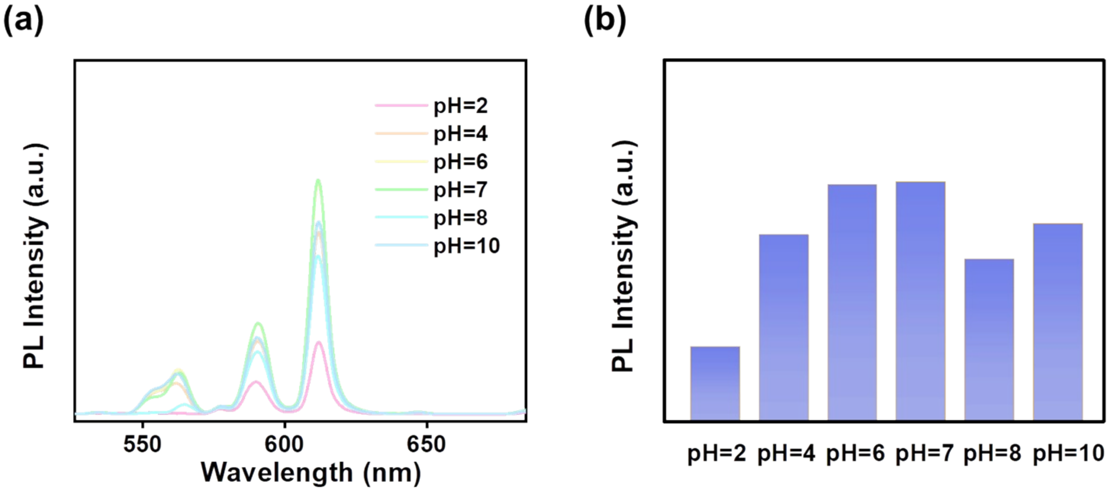

Figure S13. PL spectra (a) and intensities (b) of Eu-DPA with different pH.

Figure S14. Photographs of Eu-DPA after added different amines in aqueous solution.

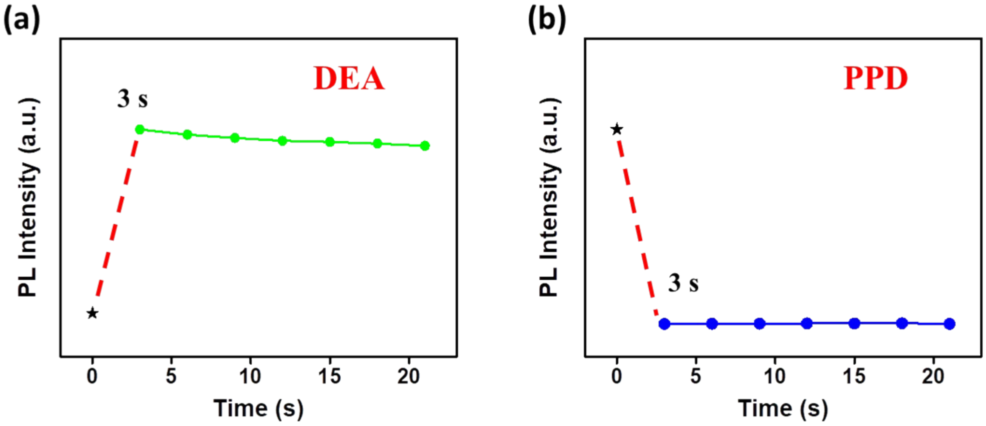

Figure S15. Fluorescence response time of Eu-DPA toward DEA (a) and PPD (b).

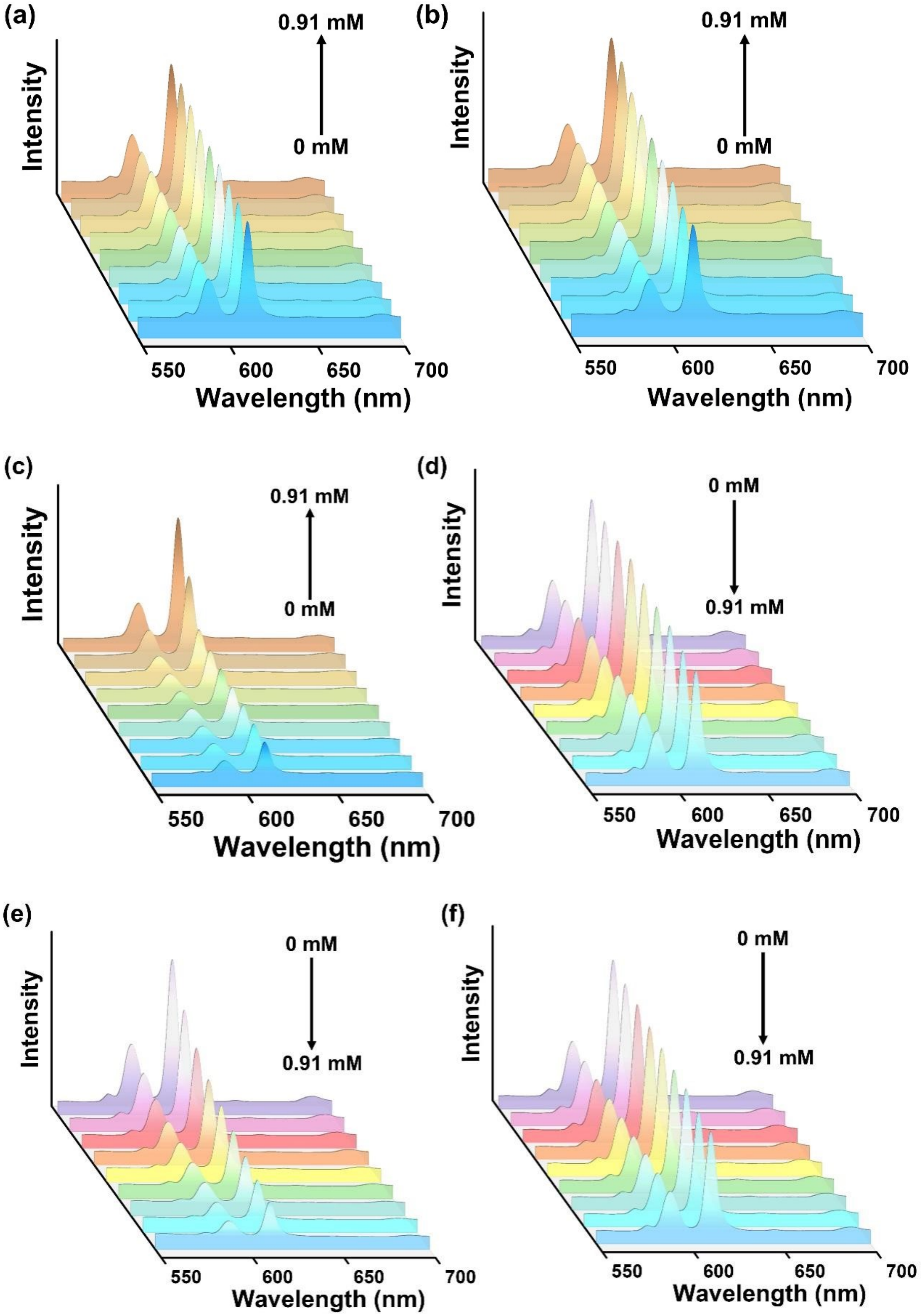

Figure S16. Fluorescence emission spectra of Eu-DPA upon the addition of different concentrations of (a) EA, (b) EDA, (c) TEA, (d) AN, (e) OPD and (f) MPD.

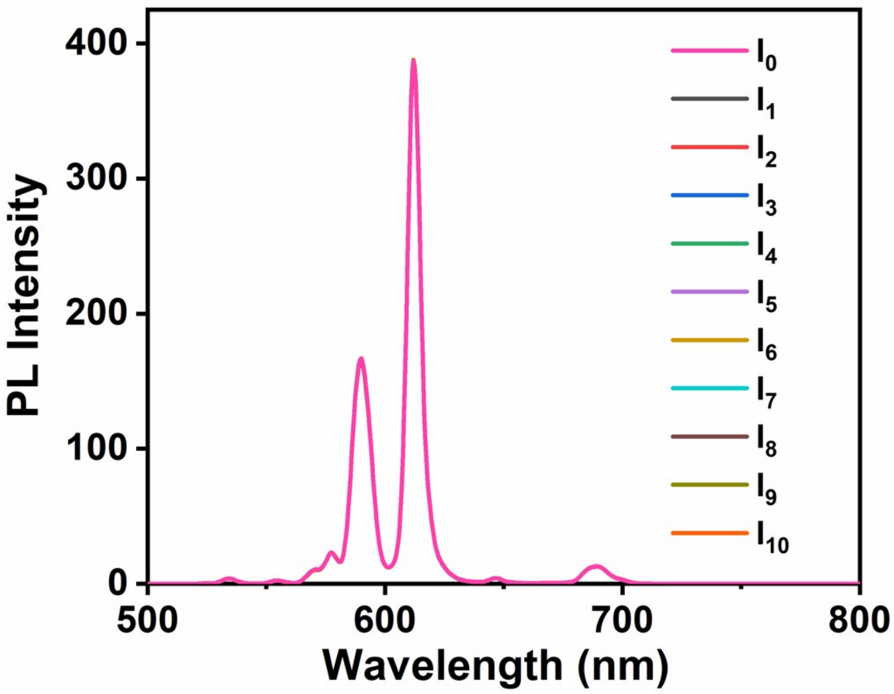

Figure S17. PL spectra of Eu-DPA for determining the standard deviation.

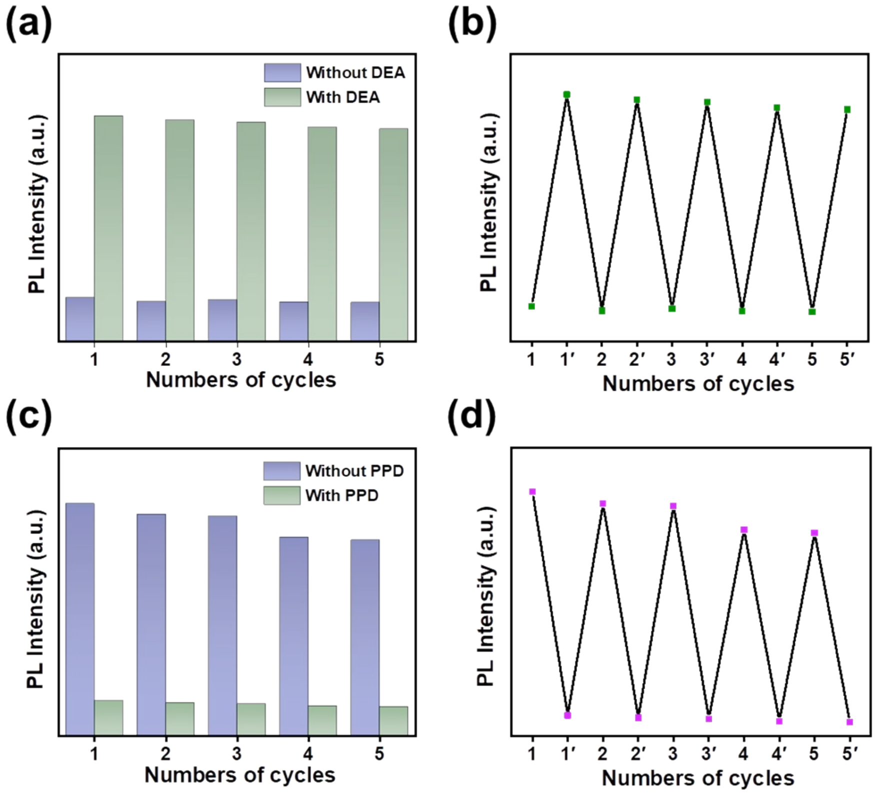

Figure S18. Recyclability experiments of Eu-DPA toward discriminative detection of DEA and PPD for 5 cycles.

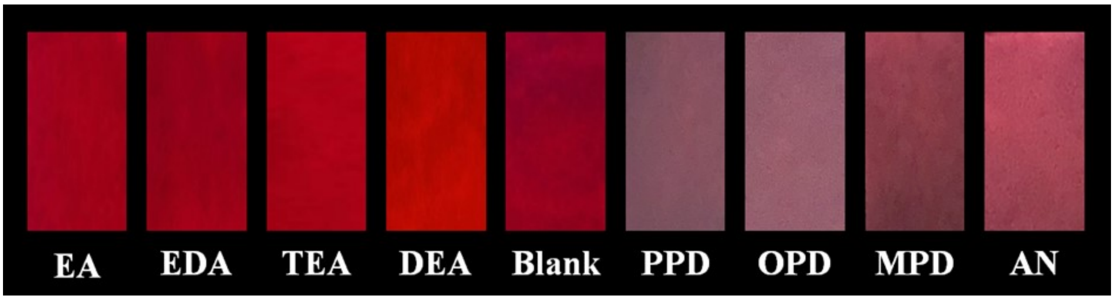

Figure S19. Photographs of test strips for blank and response to various amines under UV excitation at 254 nm.

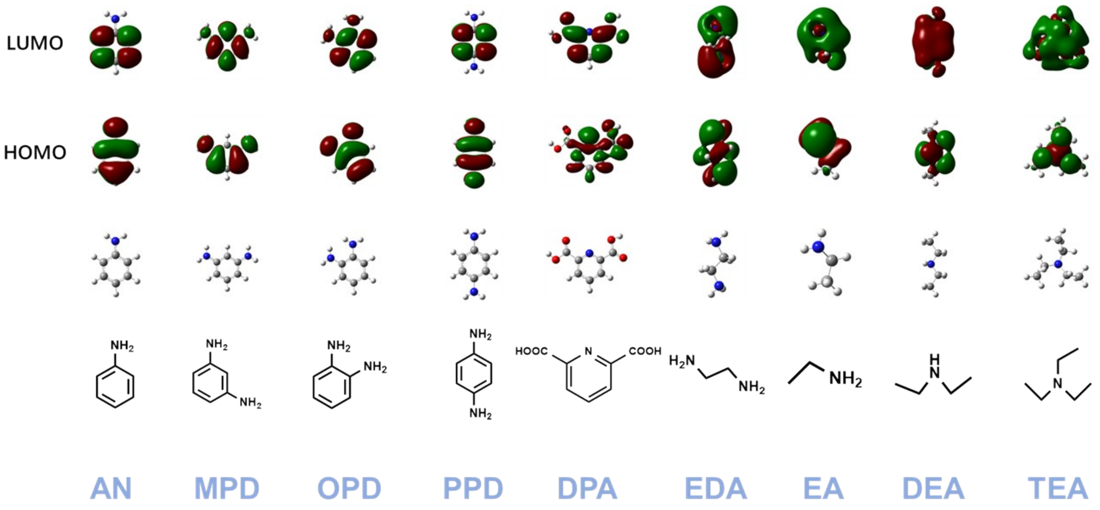

Figure S20. The ground state configurations and frontier orbital distributions of HOMO/LUMO for aromatic amines, DPA and aliphatic amines.

S-III Tables

Table S1. Fluorescence intensities and I_0/I ratios from eleven sets of PL spectra of bare Eu-DPA.

	I_0	I_1	I_2	I_3	I_4	I_5	I_6	I_7	I_8	I_9	I_{10}	σ^a
I	387.1	387.6	387.5	387.3	387.8	387.7	387.7	387.7	387.8	387.9	387.2	0.21
I_0/I	1.0000	0.9987	0.9990	0.9995	0.9982	0.9985	0.9985	0.9985	0.9982	0.9979	0.9997	$5.5x10^{-4}$

[a] the standard deviation.

Table S2. State of the art of discriminative detection of amines.

Material	**Selectivity**	**Detection limit**	**Amines amounts**	**Ref**
Eu-DPA	Aliphatic Amine (turn on) and aromatic amine (turn off)	DEA (220 nM), PPD (0.33 µM)	8	Our works
Conjugated Porous polymers (CPPs) P1 and P2	Aliphatic Amine (turn on) and aromatic amine (turn off）	TEA (43 nM), AN (81 nM)	3	1
Conjugated polymer	Aliphatic Amine (turn on) and aromatic amine (turn off)	PPD (89 µM)	8	2
Zr(IV) based MOF	Aliphatic Amine (turn on) and aromatic amine (turn off)	MA (66.2 nM), AN (0.16 µM)	5	3
BITSH-1 and BITSH-2	Aliphatic Amine (turn off) and aromatic amine（turn on）	TEA (0.66 µM), AN (2.28 µM)	5	4
$[Eu_2(BINDI)(NO_3)_2(DMA)_4]\cdot 2DMA$	OPD	0.94 µM	-	5
NH_2 -MIL-101(Fe)	PPD	1 µM	-	6
SHSPCs	DEA	68 nM	-	7
$\{[Zn_3(L)_{1.5}(DMF)_3]\bullet C_2H_7N\}n$	TEA	1.07 µM	-	8
Eu-TTPDC	EA	1.30 µM	-	9
$\{[Eu_4(taip)_4(ox)(OH)_2(H_2O)_4]\cdot 3H_2O\}n$	DEA	0.49 µM	-	10
TGH^+•PD	NH_3	0.12 µM	-	11
N-4, N-12, and N-18	TEA	2.23 µM	-	12
Tb-BTC	DEA	2 µM	-	13
Tb-TDPAT	OPD	greater than 7.5 µM	-	14
Mn-HCPCP@H4TBAPy	OPD	1.24 µM	-	15

S-IV References

[1] J. Yu and C. Zhang, *J. Mater. Chem. C.*, 2020, **8**, 16463-16469.

[2] Y. Zhao, K. Miao, Z. Zhu and L. Fan, *ACS Sens*., 2017, **2**, 842-847.

[3] A. Mallick, A. M. El-Zohry, O. Shekhah, J. Yin, J. Jia, H. Aggarwal, A. H. Emwas, O. F. Mohammed and M. Eddaoudi, *J. Am. Chem. Soc.*, 2019, **141**, 7245-7249.

[4] T. Leelasree, M. Dixit and H. Aggarwal, *Chem. Mater*., 2023, **35**, 416-423.

[5] R. Huo, C. Wang, M. Wang, M. Sun, S. Jiang, Y. Xing and F. Bai, *Inorg. Chem*., 2023, **62**, 6661−6673.

[6] Y. Xia, K. Sun, Y. Zuo, S. Zhu and X. Zhao, *CCS Chem.*, 2022, **33**, 2081–2085.

[7] L. Li, J. Li, T. Meng, Z. Liu, H. Zhou, J. Zhu and J. Shi, *Anal. Methods*., 2021, **13**, 2189–2195.

[8] L. Wang, J. Wang, E. Yue, J. Li, L. Tang, X. Wang, X. Hou, Y. Zhang, Y. Ren and X. Chen, *Dyes Pigm*. 2022, **197**, 109863.

[9] Y. Wang, C. Liu, H. Zhi, X. Zhang, Y. Xu, Y. Wang, R. Yang and X. Yin, *Chem. Eng. J.*, 2022, **441**, 136049.

[10] J. Wang, J. Fu, Y. Zhang, J. Liang, R. Zhou, S. Gong and J. Song, *Dalton Trans*., 2023, **52**, 136.

[11] G. Das, B. Garai, T. Prakasam, F. Benyettou, S. Varghese, S. K. Sharma, F. Gándara, R. Pasricha, M. Baias, R. Jagannathan, N. Saleh, M. Elhabiri, M. A. Olson and A. Trabolsi, *Nat. Commun.*, 2022, **13**, 1.

[12] X. Cao, Y, Li, A. Gao, Y. Yu, X. Chang and X. Hei, *ACS Appl. Polym. Mater*., 2019, **1**, 1485−1495.

[13] I. Ahmed, H. J. Lee and S. H. Jhung, *J. Mol. Liq*., 2021, **344**, 117765.

[14] Y. Xiao, B. Li, Z. You, Y. Xing, F. Bai, L. Sun and Z. Shi, *J. Mater. Chem. C*., 2021, **9**, 3193.

[15] M. Lv, F. Bai, G. Zeng, Z. You, Y. Xing and Z. Shi, *Cryst. Growth Des*., 2021, **21**, 6824−6839.